Biochemical and Biophysical Research Communications 425 (2012) 393–397

Contents lists available at SciVerse ScienceDirect

Biochemical and Biophysical Research Communications

journal homepage: www.elsevier.com/locate/ybbrc

Superparamagnetic iron oxide nanoparticles as radiosensitizer via enhanced reactive oxygen species formation

Stefanie Klein [a], Anja Sommer [a], Luitpold V.R. Distel [b], Winfried Neuhuber [c], Carola Kryschi [a,*]

[a] Department of Chemistry and Pharmacy, Physical Chemistry I and ICMM, Friedrich-Alexander University of Erlangen-Nuremberg, Egerlandstr. 3, D-91058 Erlangen, Germany
[b] Department of Radiation Oncology, Friedrich Alexander University Erlangen-Nuremberg, Universitätsstraße 27, D-91054 Erlangen, Germany
[c] Department of Anatomy, Chair of Anatomy I, Friedrich Alexander University Erlangen-Nuremberg, Krankenhausstr. 9, D-91054 Erlangen, Germany

ARTICLE INFO

Article history:
Received 17 July 2012
Available online 27 July 2012

Keywords:
Fenton reaction
Haber–Weiss reaction
Radiosensitizer
Reactive oxygen species
Superparamagnetic iron oxide nanoparticles

ABSTRACT

Internalization of citrate-coated and uncoated superparamagnetic iron oxide nanoparticles by human breast cancer (MCF-7) cells was verified by transmission electron microscopy imaging. Cytotoxicity studies employing metabolic and trypan blue assays manifested their excellent biocompatibility. The production of reactive oxygen species in iron oxide nanoparticle loaded MCF-7 cells was explained to originate from both, the release of iron ions and their catalytically active surfaces. Both initiate the Fenton and Haber–Weiss reaction. Additional oxidative stress caused by X-ray irradiation of MCF-7 cells was attributed to the increase of catalytically active iron oxide nanoparticle surfaces.

1. Introduction

Superparamagnetic iron oxide nanoparticles (SPIONs) are in the focus of intense research activities because of their current potential as contrast agents for magnetic resonance imaging [1,2] and colloidal mediators for cancer magnetic hyperthermia [3,4]. Other promising biomedical applications of SPIONs are multimodal biomedical imaging, targeted drug delivery and cell separation techniques [1,5–8]. SPIONs are mono-crystalline nanoparticles with sizes much smaller than the Weiss domain and have, for instance, a magnetite (Fe_3O_4) or a maghemite (γFe_2O_3) structure. Their use in diagnosis and therapy arises from two essential properties: their superparamagnetism [4,9,10] and their excellent biocompatibility [7,11]. Superparamagnetism enables to guide SPIONs to the tumor area through an external inhomogeneous magnetic field, whereas the biocompatibility and effective biodistribution of SPIONs allow for their medical application. Weissleder et al. reported on metabolism of SPIONs intravenously administered in rats [12]. The SPIONs were observed to be cleared out by the mononuclear phagocyte system that comprises bone marrow progenitors, blood monocytes and tissue macrophages such as Kupffer cells in the liver. Intracellular nanoparticles are degraded in the macrophage lysosomal compartment. The iron of the SPIONs is incorporated into the body's iron store and progressively accumulated in the hemoglobin of erythrocytes [2,3,12]. Although iron cations are essential for normal cell cycle and growth, the uptake of SPIONs can lead to a concentration increase of intracellular unbound iron, which may result into cell injury or death [12]. Recent *in vitro* cytotoxicity studies revealed some adverse effects of SPIONs which depend on their composition such as Fe_3O_4, γFe_2O_3 or Fe_2O_3. While γFe_2O_3 nanoparticles exhibit no apparent cytotoxicity, the Fe_3O_4 nanoparticles as containing Fe^{2+} ions were found to be cytotoxic. Moreover, surface chemistry and sizes of SPIONs may play essential roles for cytotoxicity. Coated SPIONs are significantly less toxic than uncoated ones [13–15]. A potential mechanism of SPION cytotoxicity involves the formation of reactive oxygen species (ROS) such as hydrogen peroxide, hydroxyl radical, hydroperoxyl radical and superoxide anion (e.g. H_2O_2, $OH^{\cdot}$, $HO_2^{\cdot}$, O_2^{-}) which provides oxidative stress [14,16]. When endocytosed into tumor cells incompletely coated or uncoated SPIONs may stimulate the generation of ROS via different pathways. One occurs through the release of iron ions into the cytosol where immediate chelation by citrate or adenosine phosphate will take place [15–18]. The chelated iron ions can participate in the Haber–Weiss chemistry and thus, catalyze the formation of the highly reactive $OH^{\cdot}$ that damages cellular membranes, proteins and DNA. The other pathway involves SPION surfaces that may act as catalyst for the Haber–Weiss cycle and therewith, for the Fenton reaction. Voinov et al. [13] reported that γFe_2O_3 nanoparticle surfaces catalyze in aqueous H_2O_2 solution the Haber–Weiss cycle

Abbreviations: DCF, 2′,7′-dichlorofluorescein; DCFH-DA, 2′,7′-dichlorodihydrofluorescein diacetate; DMEM, Dulbecco's modified eagle medium; ICP-AES, inductive coupled plasma atomic emission spectrometer; (HR)TEM, (high resolution) transmission electron microscopy; ROS, reactive oxygen species; SPION, superparamagnetic iron oxide nanoparticle.

* Corresponding author. Address: Department of Phsical Chemistry I, Friedrich-Alexander University of Erlangen-Nuremberg, D-91058 Erlangen, Germany. Fax: +49 91318528967.
E-mail address: kryschi@chemie.uni-erlangen.de (C. Kryschi).

0006-291X/$ - see front matter © 2012 Elsevier Inc. All rights reserved.
http://dx.doi.org/10.1016/j.bbrc.2012.07.108

which starts via the superoxide-driven reduction of Fe^{3+} to Fe^{2+} and results into the formation of highly reactive $OH^{\cdot}$. They could show that surface Fe^{3+} ions are at least 50-fold more efficient for the hydroxyl radical production than dissolved Fe^{3+} ions. In our opinion, this catalytic effect of incompletely coated SPIONs has a promising potential for cancer therapy, in particular for radiotherapy. The principle of radiotherapy is based on the application of ionizing radiation for destroying tumor tissues in cancer patients. One kind of ionizing radiation are X-rays that damage cellular compartments as well as decompose and ionize water molecules which results into the formation of ROS. SPIONs may increase the therapeutic efficiency of radiotherapy by catalyzing and, thereupon, enhancing X-ray induced ROS production. The catalytic effect promises to treat cancer patients with significantly decreased total radiation doses which minimize painful side effects of ionizing radiation.

So far, the application of SPIONs as radiosensitizer for cancer therapy remains unexplored [19,20]. In this contribution, we present novel results obtained from *in vitro* studies of the formation of ROS in SPION loaded MCF-7 cells which were exposed to X-rays or left non-irradiated. All studies presented here were performed with uncoated or citrate-coated SPIONs and Fe^{2+} or Fe^{3+} ions, where the latter were used as reference systems. We could show that in particular, incompletely citrate-coated SPIONs may function as excellent radiosensitizer upon enhancing the impact of X-rays on the ROS generation for about 240%.

2. Materials and methods

2.1. Chemicals

$FeCl_3{\cdot}6H_2O$ (99%, Acros organics), $FeCl_2{\cdot}4H_2O$ (99%, Sigma–Aldrich) and citric acid anhydrous (99.5%, Alfa Aesar) were used as received. Dulbecco's modified eagle medium (DMEM), L-glutamine, fetal calf serum (FCS), penicillin–streptomycin-solution, sodium pyruvate, phosphate buffered saline (PBS), non-essential amino acids (MEM), trypsin/ethylendiamine (EDTA), 3-(4,5-dim-ethythiazol-2-il)-2,5-diophenyltetrazolium bromide) (MTT) (98%), trypan blue solution (0.4%) and 2′,7′-dichlorofluorescein diacetate (DCFH-DA) (95%) were purchased from Sigma–Aldrich and glutaraldehyde (25%) from Roth. DCFH-DA was dissolved in dimethyl sulfoxide (99.7%, Baker, Deventer, Netherlands) to obtain a stock solution (0.01 M) and was kept frozen at −20 °C. For loading the cells with DCFH-DA the stock solution was mixed with DMEM to a final concentration of 100 μM.

2.2. Syntheses of SPIONs

There are two synthesis procedures applied here to prepare uncoated and citrate-coated SPIONs. One uses co-precipitation of ferric and ferrous chlorides in alkaline aqueous solution at low temperature (0 °C) and follows Massarís method [21]. The other consists of a high temperature one-pot alkaline co-precipitation in diethylene glycol at 220 °C which is followed by a ligand exchange reaction step [22].

2.3. Cell culture

The human breast cancer cells (MCF-7) were cultured in DMEM containing 4500 mg Glucose/L, which was enriched with 10% FCS, 1 mM sodium pyruvate, 100 μ/mL penicillin–streptomycine solution, 100 μg/mL streptomycin, 2 mM L-glutamine and 1% MEM. In a humidified environment of 5% CO_2 at 37 °C the cells were incubated and subcultivated twice a week.

2.4. Transmission electron microscopy

MCF-7 cells were incubated for 24 h with cell culture medium containing SPIONs at a concentration of 0.1 mg Fe/mL. Cells were washed with PBS and fixed with 2.5% glutaraldehyde overnight at 4 °C and then postfixed in 1% osmium tetroxide and 3% potassium ferricyanide at room temperature. The cells were dehydrated, embedded in Epon and mounted on Epon blocks. Silver–grey ultrathin sections were contrasted with uranyl acetate and were imaged using a Zeiss 906 transmission electron microscope (LEO, Germany).

2.5. Cell viability assay

The trypan blue exclusion test is used to determine the number of viable cells. MCF-7 cells were incubated with SPIONs for definite periods (1, 24, 48, 72 h). Cell suspensions of 10^5 cells/mL were placed in a test tube. After adding trypan blue the solution was extensively mixed and allowed to stand for several minutes. Finally the cells were counted in a hemocytometer.

2.6. Metabolic assay

The MTT assay is based on the ability of viable cells to reduce the soluble yellow tetrazolium salt to purple formazan crystals. MCF-7 cells were seeded in a 96 well-plate at a density of 10^3 cells per well. After 3 days the cell culture medium was replaced with one containing SPIONs at a concentration of 0.1 mg Fe/mL. One part of the wells, the control wells, was left with medium without SPIONs. There were two examples created for the wells containing SPIONs, one is used as sample well (SPIONs with MTT solution) and the other serves as reference well (SPIONs without MTT solution). After 1, 24, 48 and 72 h incubation the medium was removed and 50 μL of the MTT solution (0.5 mg/mL in PBS) was added to each sample well. The solution was removed after 1 h and the formazan crystals were solubilized with 100 μL DMSO. The metabolic activity was determined by measuring the absorbance of the formazan solution at 590 nm. The relative cell viability (%) was calculated by subtracting the absorbance of the reference well solution from that of the sample well solution and by subsequent division of the resulting difference by the absorbance of the control well solution.

2.7. Radiation experiments

MCF-7 cells were cultivated in 96 well-plates at a density of 10^3 cells/well and were allowed to grow for 3 days. After removing the medium, the cells were incubated for 24 h with different cell culture media that contain either SPIONs (0.1 mg Fe/mL), iron salts (0.1 mg Fe/mL) or citric acids (0.169 mol/L). Afterwards the cells were washed with PBS and loaded with 100 μM DCFH-DA in DMEM for 30 min. Each well was loaded with 100 μL PBS, and one half of the plate was irradiated with X rays using a 120 kV X-ray tube (Isovolt, Seifert, Germany) at a single dose of 3 Gy. ROS species oxidize intracellular DCFH to the fluorescent DCF dye. The DCF fluorescence intensity is directly proportional to the ROS concentration. The DCF fluorescence spectrum of each well was recorded on a Jobin–Yvon FluoroMax-3 spectrofluorometer. The fluorescence emission was excited at 480 nm and recorded between 500 and 700 nm. The relative fluorescence intensity was determined by integrating the spectrum. The intensity values were related to those obtained from fluorescence measurements of cells in the pure culture medium.

2.8. Statistical analysis

Data are presented as arithmetic mean values ± standard error. Statistical analysis was performed using the analysis of variance

(ANOVA) with *post hoc* Bonferroni correction for multiple comparisons. A value of $p < 0.05$ was considered being statistically significant.

3. Results and discussion

Two different synthesis routes were used to prepare uncoated and citrate-coated SPIONs. According to XRD data both, the high-temperature (HT) and low-temperature (LT) procedures yielded mono-crystalline SPIONs. While HT-SPIONs consist of mixed crystals with a maghemite (γFe_2O_3) and magnetite (Fe_3O_4) structure, LT-SPIONs have a maghemite structure, only. As visualized by HRTEM images the predominantly polygonal SPIONs (Fig. 1(a)) exhibit a size distribution between 6 and 20 nm, while the size distribution of the spherical HT-SPIONs (Fig. 1(b)) ranges between 3 and 10 nm.

The cellular uptake of SPIONs was verified upon TEM imaging. The most probable entry mechanism for SPIONs is endocytosis which is clearly demonstrated in Fig. 2(a)–(e). For comparison a TEM image of a MCF-7 cell without SPIONs is presented in Fig. 2(a), whereas the TEM images in Fig. 2(b) and (c) show MCF-7 cells that contain either LT-SPIONs or HT-SPIONs. As visualized in Fig. 2(d), an endocytic carrier vesicle filled with SPIONs was transported into the cytoplasm along the endosomal pathway toward the lysosomes. In the cytosol the SPIONs accumulate around the membranes of lysosomes wherein their degradation will take place (Fig. 2(e)).

The concentration of LT- and HT-SPION solution was determined using ICP-AES in order to prepare a cell culture medium that contains iron ions at the concentration of 0.1 mg/mL.

The influence of intracellular SPIONs on the viability of MCF-7 cells was evaluated using the trypan blue assay, while MTT reduction was used to quantify metabolically active cells. Fig. 3(a) shows the relative cell viability (%) of MCF-7 cells exposed to uncoated and citrate-coated LT- and HT-SPIONs for 1 to 72 h, which was compared with cell culture medium containing citric acid. The number of unstained MCF-7 cells that were cultivated with differently synthesized SPIONs reached values higher than 90% for incubation times up to 72 h. A somewhat decreased percentage of viable cells (87%) were found for uncoated LT-SPIONs after 72 h. In case of citric acid the decreased value is explained with its detaching effect on MCF-7 cells. Next to the cell viability the metabolic activity had been studied, since the majority of ROS are products of the mitochondrial respiration in aerobe cells. Fig. 3(b) and (c) show the relative metabolic activity of MCF-7 cells which is related to control cells without nanoparticles. For LT-SPIONs the metabolic activity increased with rising incubation time from 80% (1 h) to values between 90% and 100 % after incubation for 72 h (Fig. 3(b)). Very similar results were obtained for uncoated HT-SPIONs, whereas incubation in presence of citric acid was observed to result into a drastic reduction of metabolic activity (Fig. 3(a)). According to these results both, LT- and HT-SPIONs, exhibit a negligibly small influence on the metabolic activity of MCF-7 cells. These toxicology studies verified good biocompatibility of the SPIONs studied here.

Our major objective was to quantify and understand the radio-enhancing effect of internalized LT- and HT-SPIONs. Since X-ray treatment of tumor cells is associated with enhanced formation of ROS, the ROS concentration in MCF-7 cells was measured to determine the efficiency of intracellular SPIONs for ROS formation. Therefore, MCF-7 cells were incubated with uncoated or citrate-coated LT- and HT-SPIONs and exposed to X-rays at a single dose of 3 Gy or left non-irradiated (Fig. 4(a)). The ROS concentration was measured via the fluorescence intensity of DCF that emerges due to quantitative oxidation of internalized non-fluorescent DCFH per mole ROS. The 100% value of the fluorescence intensity refers to X-ray exposed MCF-7 cells without SPIONs (Fig. 4(a)). The white bars present the relative fluorescence intensity values of non-irradiated MCF-7 cells containing SPIONs, whereas MCF-7 cells cultivated with the different SPION species and exposed to X-rays exhibit fluorescence intensity values (black bars).

Obviously, all internalized SPION species resulted into an enhancement of ROS formation and the enhancing effect of the X-ray treatment is as well manifest. In particular, citrate-coated LT-SPIONs in X-ray treated MCF-7 cells exhibit a fluorescence intensity of 340%, which indicates an enhancement in ROS formation for 240% when compared with X-ray treated cells without internalized SPIONs. However, even LT-SPIONs internalized in non-irradiated cells cause a relative increase of ROS concentration up to 77%. This implies that SPIONs do not only enhance the efficiency of X-rays on ROS formation. They also may act via their surfaces as catalyst for the Haber–Weiss cycle and moreover, contribute via releasing iron ions to the generation of ROS through the Haber–Weiss and Fenton reaction. To quantify the contribution of intracellular iron ions to the ROS formation, MCF-7 cells were incubated with Fe^{2+} or Fe^{3+} solutions. As before, the ROS concentration of X-ray irradiated and non-irradiated MCF-7 cells were determined by measuring the fluorescence intensity of the ROS probe dye DCF (Fig. 4(b)). The non-irradiated MCF-7 cells that contain Fe^{2+} or Fe^{3+} ions exhibit relatively smaller ROS concentrations (Fig. 4(b), black bars) when compared to the reference MCF-7 cells

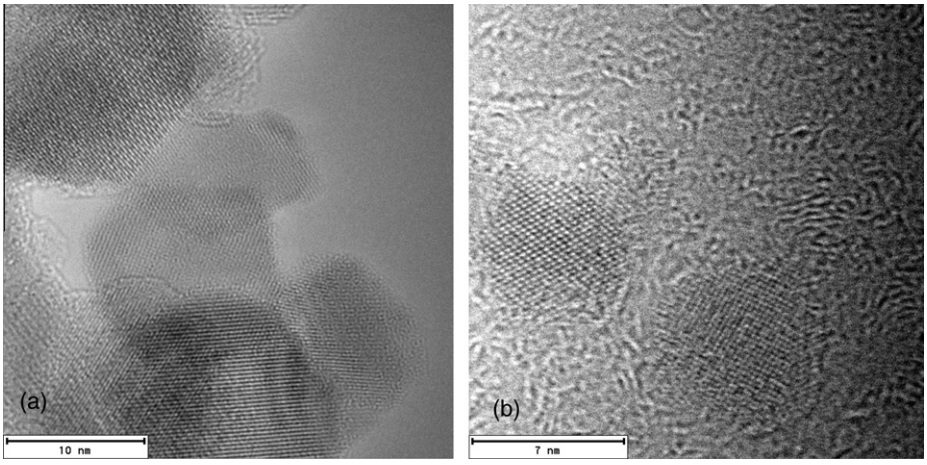

Fig. 1. HRTEM images of LT-SPIONs (a) and HT-SPIONs (b).

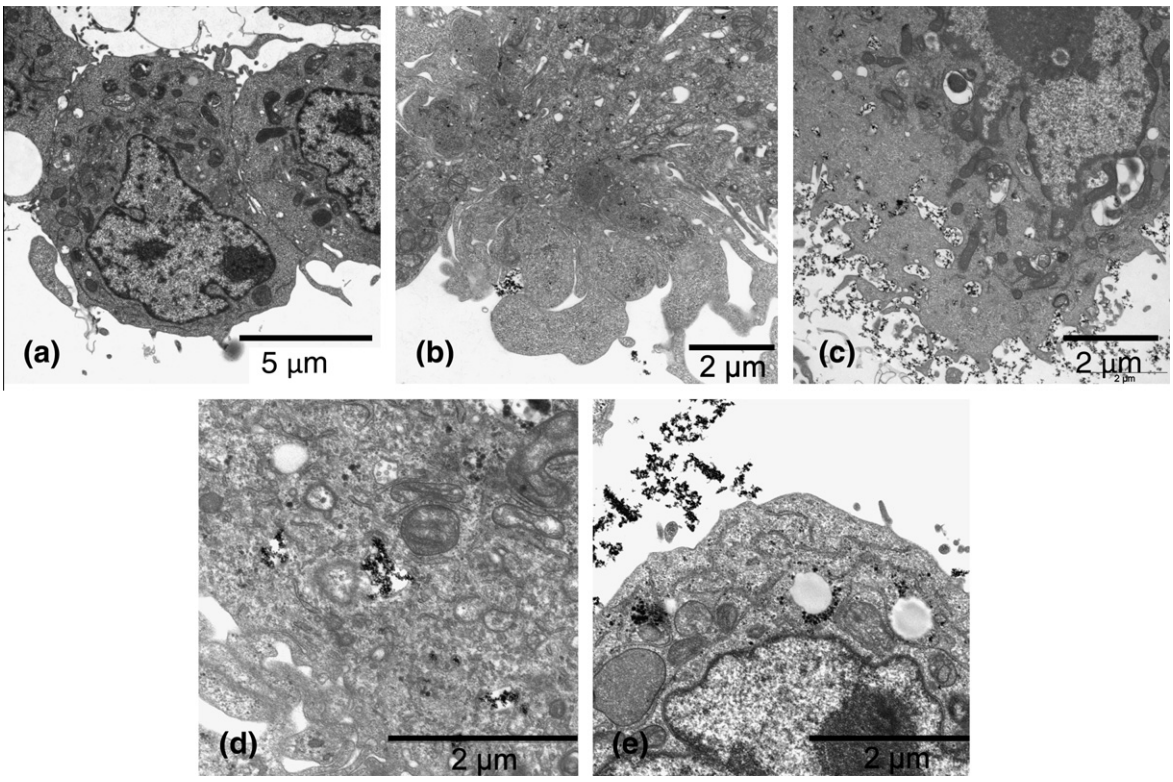

Fig. 2. The TEM images of ultrathin sections of MCF-7 cells without SPIONs (a) and of those loaded with SPIONs illustrate the endocytosis of LT-SPIONs (b) and HT-SPIONs (c), where an endocytic carrier vesicle is filled with LT-SPIONs (d), and the accumulation of LT-SPIONs around the membranes of lysosomes (e).

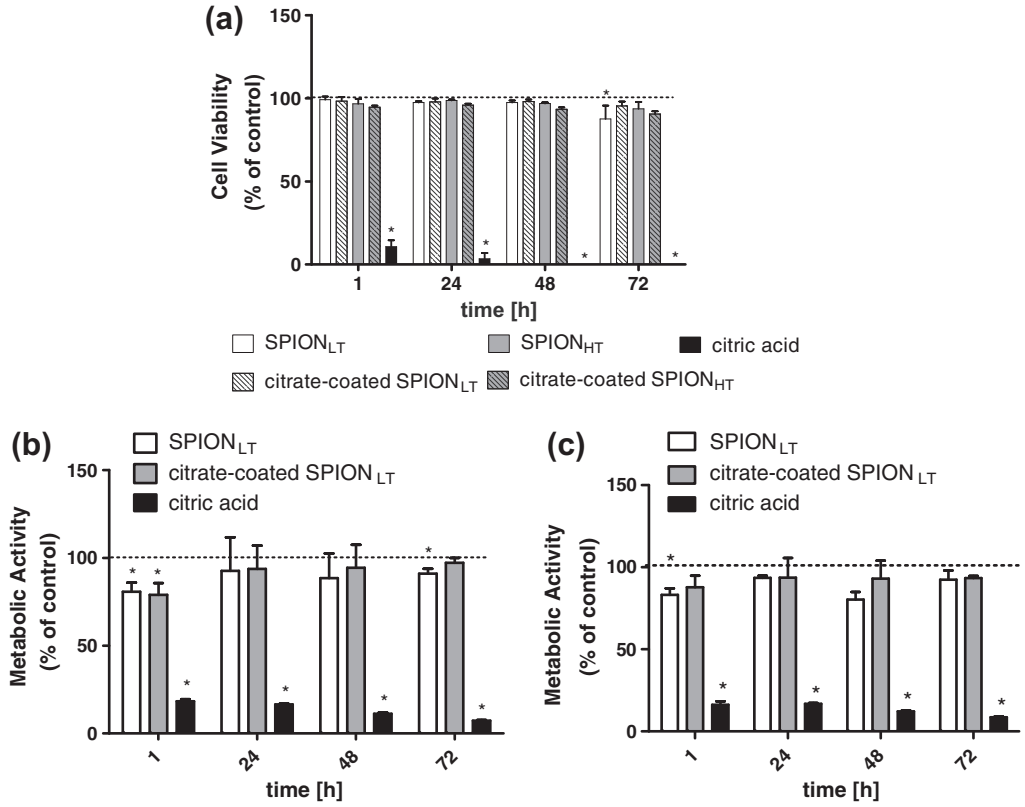

Fig. 3. The biocompatibility of SPIONs was tested using the trypan blue assay (a) and MTT assay (b)(c): the relative cell viability of MCF-7 cells (%) loaded with citric acid, uncoated or citrate-coated LT- and HT-SPIONs (a) and the metabolic activity (%) of MCF-7 cells loaded with citric acid, uncoated or citrate-acid coated LT-SPIONs (b) and HT-SPIONs (c); $n = 4$, $^{*}p > 0.05$.

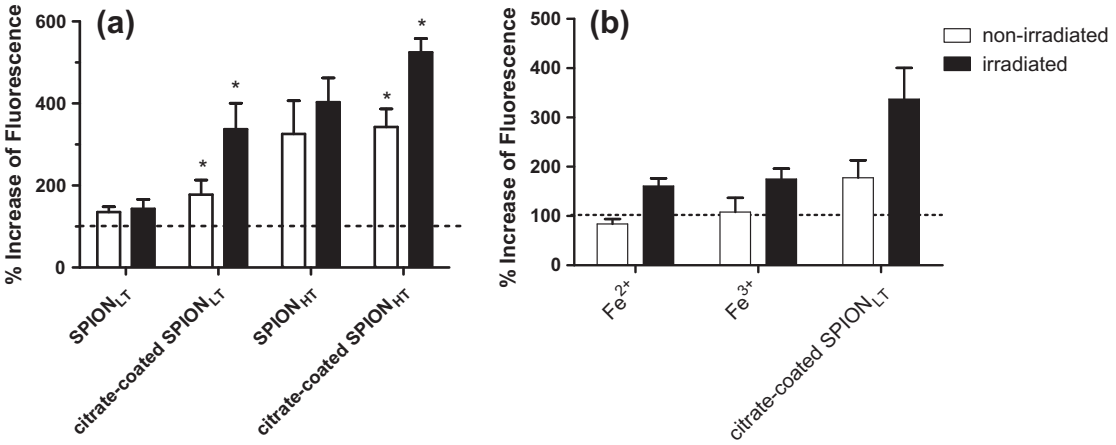

Fig. 4. Determination of relative ROS concentration in X-ray irradiated and non-irradiated MCF-7 cells loaded with uncoated and citrate-coated LT- and HT-SPIONs (a) and determination of relative ROS concentration in X-ray irradiated and non-irradiated MCF-7 cells loaded with Fe^{2+}, Fe^{3+} or citrate-coated LT-SPIONs (b) using the DCFH-DA assay: the values of relative ROS concentration are represented as increase of DCF fluorescence intensity (%); $n = 6$, $^{*}p > 0.05$.

(broken line at 100%). X-ray exposure of Fe^{2+} or Fe^{3+} incubated MCF-7 cells was observed to result into an increase of relative ROS concentration for 60% to 75% (black bars). For comparison, the relative ROS concentration in X-ray exposed MCF-7 cells with internalized citrate-coated LT-SPIONs is 4-fold larger than that of non-irradiated MCF-7 cells with internalized Fe^{2+} ions. On the other hand, the relative ROS concentration of non-irradiated MCF-7 cells approximately reaches that value of non-irradiated MCF-7 cells containing Fe^{3+} ions. Obviously, intracellular citrate-coated SPIONs significantly outclass iron ions with respect of X-ray induced ROS formation in MCF-7 cells. This enhancing effect of citrate-coated SPIONs is explained with the impact of high-energy X-rays onto the SPION surfaces due to efficient destruction of surface structures. The surface coverage either consisting of adsorbed citrate molecules, water or hydroxyl ions is partially destroyed due to X-ray irradiation. The freed SPION surface, containing now easier accessible iron ions, should act as a more efficient catalyst for ROS production than completely coated surface. In comparison with the HT-SPIONS the LT-SPIONs show a relatively low ROS formation for non-irradiated cells and therefore exhibit a promising potential as radiosensitizer.

Acknowledgments

Support of the Deutsche Forschungsgemeinschaft (GRK 1161/2) is gratefully acknowledged. We thank Andrea Hilpert for TEM imaging studies. Sincere thanks are given to PD Dr. Oliver Zolk (Institute of Experimental and Clinical Pharmacology and Toxicology, University of Erlangen-Nuremberg) for generously supporting our cell viability assay experiments. Furthermore, we are grateful to Regina Müller (Prof. Dr. Peter Wasserscheid, CRT, University of Erlangen-Nuremberg) for conducting so diligently the ICP-AES experiments.

References

[1] C. Sun, J.S.E. Lee, M. Zhang, Magnetic nanoparticles in MR imaging and drug delivery, Adv. Drug Delivery Reviews 60 (2008) 1252–1265.
[2] A.S. Arbab, L.A. Bashab, B.R. Miller, E.K. Jordan, B.K. Lewis, H. Kalish, J.A. Frank, Characterization of biophysical and metabolic properties of cells labeled with superparamagnetic iron oxide nanoparticles and transfection agent for cellular MR imaging, Radiology 229 (2003) 838–846.
[3] S. Mornet, S. Vasseur, F. Grasset, E. Duguet, Magnetic nanoparticle design of medical diagnosis and therapy, J. Mater. Chem. 14 (2004) 2161–2175.
[4] N. Tran, T.J. Webster, Magnetic nanoparticles: biomedical applications and challenges, J. Mater. Chem. 20 (2010) 8760–8767.
[5] Q.A. Pankhurst, J. Connolly, S.K. Jones, J. Dobson, Applications of magnetic nanoparticles in biomedicine, J. Phys. D, Appl. Phys. 36 (2003) R167–R181.
[6] L. Frullano, T.J. Meade, Multimodal MRI contrast agents, J. Biol. Inorg. Chem. 12 (2007) 939–949.
[7] A.S. Lubbe, C. Alexiou, C. Bergemann, Clinical applications of magnetic drug targeting, J. Surgical Res. 95 (2001) 200–206.
[8] M.K. Yu, Y.Y. Jeong, J. Park, S. Park, J.W. Kim, J.J. Min, K. Kim, S. Jon, Drug-loaded superparamagnetic iron oxide nanoparticles for combined cancer imaging and therapy in vivo, Angew. Chem. Int. Ed. 47 (2008) 5362–5365.
[9] A. Petri-Fink, M. Chastellain, L. Juillerat-Jeanneret, A. Ferrari, H. Hofmann, Development of functionalized superparamagnetic iron oxide nanoparticles for interaction with human cancer cells, Biomaterials 26 (2005) 2685–2694.
[10] E.K. Schlachter, H.R. Widmer, A. Bregy, T. Lönnfors-Weitzel, I. Vajtai, N. Corazza, V.J.P. Bernau, T. Weitzel, P. Mordasini, J. Slotboom, G. Herrmann, S. Bogni, H. Hofmann, M. Frenz, M. Reiner, Metabolic pathway and distribution of superparamagnetic iron oxide nanoparticles: in vivo study, Int. J. Nanomedicine 6 (2011) 1793–1800.
[11] J.S. Kim, T.-J. Yoon, K.N. Yu, B.G. Kim, S.J. Park, K.H. Lee, S.B. Park, J.-K. Lee, M.H. Cho, Toxicity and tissue distribution of magnetic nanoparticles in mice, Toxicol. Sci. 89 (2006) 338–347.
[12] R. Weissleder, D.D. Stark, B.L. Engelstad, B.R. Bacon, C.C. Compton, D.L. White, P. Jacobs, J. Lewis, Superparamagnetic iron oxide: pharmacokinetics and toxicity, Am. J. Roentgenol. 152 (1989) 167–173.
[13] M.A. Voinov, J.O.S. Pagan, E. Morrison, T.I. Smirnova, A. Smirnov, Surface-mediated production of hydroxyl radicals as a mechanism of iron oxide nanoparticle biotoxicity, J. Am. Chem. Soc. 133 (2011) 35–41.
[14] N. Lewinski, V. Colvin, R. Drezek, Cytotoxicity of nanoparticles, Small 4 (2008) 26–49.
[15] M. Auffan, W. Achouak, J. Rose, M.-A. Roncato, C. Chaneac, D. T. Waite, A. Masion, J. C. Woicik, M. R. Wiesner J.-Y. Bottero, Relation between the redox state of iron-based nanoparticles and their cytotoxicity toward *Escherichia coli*, Environ. Sci. Technol. 42 (2008) 6730–6735.
[16] A. Nel, T. Xia, L. Mädler, N. Li, Toxic potential of materials at the nanolevel, Science 311 (2006) 622–627.
[17] J. Emerit, C. Beaumont, F. Trivin, Iron metabolism, free radicals, and oxidative injury, Biomed. Pharmacother. 55 (2001) 333–339.
[18] M. Mahmoudi, A. Simchi, M. Imani, M.A. Shokrgozar, A.S. Milani, U.O. Häfeli, P. Stroeve, A new approach for the in vitro identification of the cytotoxicity of superparamagnetic iron oxide nanoparticles, Colloids Surf., B 75 (2010) 300–309.
[19] P. Juzenas, W. Chen, Y.-P. Sun, M.A.N. Coelho, R. Generalov, N. Generalova, I.L. Christensen, Quantum dots and nanoparticles for photodynamic and radiation therapies of cancer, Adv. Drug Delivery Rev. 60 (2008) 1600–1614.
[20] B. Halliwell, O.L. Aruoma, DNA damage by oxygen-derived species, FEBS Lett. 281 (1991) 9–19.
[21] R. Massard, Preparation of aqueous magnetic liquids in alkaline and acidic media, IEEE Trans. Magn. 17 (1981) 1247–1248.
[22] H. Qu, D. Caruntu, H. Liu, C.J. O'Connor, Water-dispersible iron oxide magnetic nanoparticles with versatile surface functionalities, Langmuir 27 (2011) 2271–2278.